JOURNAL OF SOLID STATE CHEMISTRY 114, 459–468 (1995)

Electronic Lone Pair Localization and Electrostatic Energy Calculations: Application to α-PbO, SnO, $Pb_{1-x}(TiO)_xO$, Pb_3O_4, $Pb_3(V,P)_2O_8$, and a BiSrCaCuO-Type Superconductor

D. Le Bellac,* J. M. Kiat,*,†,[1] and P. Garnier†

*Laboratoire Léon Brillouin (CEA–CNRS), Centre d'Etudes Nucleaire de Saclay, 91191 Gif-sur-Yvette Cedex, France; and †Laboratoire de chimie physique du solide (URA 453 au CNRS), Ecole Centrale des Arts et Manufactures, 92295 Châtenay-Malabry Cedex, France

Received February 8, 1994; accepted May 9, 1994

A method of calculation has been developed for localizing electronic lone pairs in crystalline structures including incommensurate modulated structures or structures containing impurities. The cohesion energy of the resulting structure (ions and lone pairs) may also be calculated. The calculation is based on the method of A. Verbaere, R. Marchand, and M. Tournoux (*J. Solid State Chem.* 23, 383, 1978), which assumes knowledge of the electronic polarizability coefficient of the ions possessing a lone pair, relative to the local electric field in the crystalline structure. These calculations have been made for some compounds and related to experimental studies. The influence of the lone pairs on the structural incommensurate transition of α-PbO is studied and compared with their influence on the structural evolution of SnO and $Pb_{1-x}(TiO)_xO$. Using the same method, the role of the lone pairs in Pb_3O_4, $Pb_3(V,P)_2O_8$, and a BiSrCaCuO-type incommensurate superconductor is discussed.

INTRODUCTION

During the past two decades, some experimental and theoretical works have been undertaken in order to understand the influence of lone pairs on the stability of some crystalline structures and on structural phase transitions. The steric effect of electronic lone pairs has been evidenced in many compounds (1–8). A lone pair refers to an electronic orbital occupied by two electrons; this orbital can be localized far from the nucleus of its ion of origin. In addition, some of the lone pairs' properties are comparable to those of an ns^2-type orbital of spherical symmetry .That is why Galy *et al.* (2) define the lone pair as an intermediate state between an inert spherical ns^2-type orbital which is centered on the nucleus,and a nonbonded hybridized-orbital lobe which is not spherical but localized far from the atomic nucleus. This orbital of two electrons is encountered in compounds containing ions with an appropriate valence such as Pb(II), Sn(II), Bi(III), and Tl(I). In those cases, because of the electronic configuration of the atoms, two electrons of the ion are not involved in any bonds. According to whether or not the local symmetry of the ion permits displacement along one direction, the two electrons occupy a shifted orbital relative to the ion position.

Many compounds possess such lone pairs in their structure. Some authors have shown that the steric occupation of the lone pairs is comparable to the steric occupation of O^{-2} or F^- ions (2–4). In the transformation of PbO_2 into PbO, for instance, it was shown that lone pairs take up positions on some O^{-2} ions' sites. More recently, some works have been completed which point out the influence of the lone pairs in structural phase transitions in lead- and bismuth-containing compounds such as Pb_3O_4, lead orthophosphovanadates, and bismuth superconductors (5–7).

All those works were based on the stereochemical properties of the lone pairs. In parallel, Verbaere *et al.* (1) proposed a description of the influence of lone pairs taking into account their electrostatic contribution. They were able to determine the position of the lone pairs in the structures of different crystals that can tolerate an ionic crystal approximation. They calculated those positions in thallium(I) oxygenated compounds and both structures of lead monoxide. Their results confirm some conclusions made from stereochemical considerations but contradict others such as the determination of the lone pairs' position in β-PbO. Thus, this method yields new quantitative information about the positions of lone pairs in different structures.

We propose in this work to use this method to analyze the electrostatic influence of lone pairs in different structures with increasing complexity. We have developed the method to be applicable to complex structures such as incommensurate structures or impurity-containing structures. We have also developed a method of calculating the electrostatic energies of the resulting structures taking

[1] To whom correspondence should be addressed.

0022-4596/95 $6.00

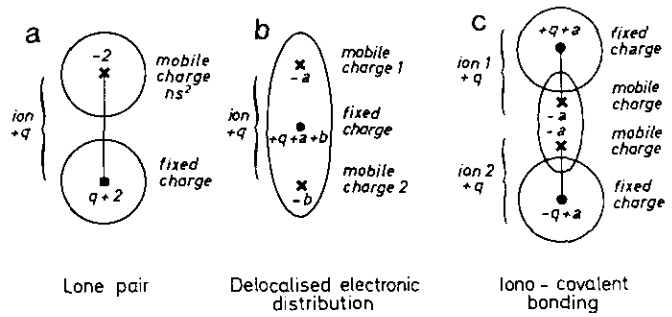

FIG. 1. Different cases of modeling that can be used in the program.

into account the calculated positions of the lone pairs. We have applied these calculations to α-PbO in order to analyze the incommensurate phase transition that occurs at 227 K. We have made some comparisons with the isostructural tin oxide SnO and the solid solution $Pb_{1-x}(TiO)_xO$, for which no phase transition occurs. Finally, we present calculations for other compounds containing lone pairs and the analyses and conclusions we can deduce from these calculations.

THEORY OF THE LOCALIZATION OF LONE PAIRS AND OF THE DETERMINATION OF THE ELECTROSTATIC ENERGY OF THE STRUCTURE OF IONIC CRYSTALLINE COMPOUNDS

We consider an infinite ionic crystal with spherical non-recovering charge distribution. The crystal is then equivalent to a punctual charge distribution (Gauss' theorem) centered on the atomic positions. In addition, we assume that each lone pair is spherical and very separate from its ion of origin. Thus, each lone pair is also equivalent to a punctual charge such as a common ion (Fig. 1a).

Lone pair localization in a crystalline structure is based on the knowledge of the electronic polarizability of its ion of origin. Indeed, under the influence of the local electric field in the crystal, ions are polarized. The delocalization of the lone pair is assumed to be due to the deformation of the electronic cloud of the ion because of that polarization. Thus, the knowledge of the coefficient of polarizability of an ion allows one to determine the position of a lone pair by finding the equilibrium state between the local electric field and the electronic polarization of an ion, i.e., the electric dipolar momentum of the distorted cloud. In an ionic crystal approximation with lone pairs equivalent to punctual charges, the electric dipolar momentum of an ion possessing a lone pair is equal to $q\boldsymbol{\delta}$, q being the electric charge of a lone pair, i.e., $-2|e|$, and $\boldsymbol{\delta}$ being the vector that links the nucleus of the ion to the center of its associated lone pair. The ion possessing a lone pair is then formed of a relative charge $q + 2$ located at the atomic position, q being the charge of the ion, and a relative charge of -2 at the position of the lone pair (Fig. 1a). The relation between the $\boldsymbol{\delta}$ vector and the local electric field $\mathbf{E}$ is then

$$q\boldsymbol{\delta} = \alpha\mathbf{E}, \qquad [1]$$

where α is the electronic polarizability of the ion. The electric field is assumed to be constant between the nucleus and the lone pair so that it can be taken on the position of the nucleus. The electronic polarizability coefficient, α, is nearly constant for a given ion whatever the ionic compound containing it (8). Thus, it can be determined by the Clausius–Masotti formula and from refraction index measurements of materials containing those ions.

The determination of the equilibrium is made by an iteration process that converges toward the equilibrium. An iteration is made up of the calculations of the local electric field for the different ions of the unit cell that possess lone pairs. Then the position of each lone pair is modified according to Eq. [1]. But as that modification of position implies modification of the local electric fields, the calculation is repeated until equilibrium is achieved between electric dipoles and local electric fields. We notice that, in the calculation of the local electric field at an ion position, the contribution of its associated lone pair must be removed because that lone pair does not contribute to the polarization of the ion. The first calculation is made using arbitrary positions of the lone pairs $\boldsymbol{\delta}^{\text{ini}}$; for instance, centered on the nucleus, where $\boldsymbol{\delta}^{\text{ini}} = 0$. This method takes into account not only the ions of the structure, but also the electrostatic influence of the lone pairs that are considered as common ions during the calculation of a local electric field.

The calculation of the local electric field is performed using Ewald's method (9), which enhances the convergence speed of the summation of the electrostatic contributions of all the ions in the crystal. This method was developed for the calculation of the electrostatic energy of an infinite ionic crystalline structure. Verbaere *et al.* (1) derived this method to calculate the local electric field at the position of an ion. The complete expression of the jth ($j = 1, 2, 3$) covariant coordinate of the local electric field at an ion p' is

$$\begin{aligned} E_j(p') = -(|e|/|a_j|) \sum_p \sum_{\mathbf{h}}{}' \{&[z_p/(\pi\Delta|\mathbf{k_h}|^2)] \\ &[\exp(-\pi^2\eta^2|\mathbf{k_h}|^2)]2\pi h_j \sin(2\pi\mathbf{k_h}(\mathbf{r}_{p'} - \mathbf{r}_p)) \\ &+ (z_p/t^2) \cdot G_j(p)[1 - F(t/\eta) \\ &+ (2t \exp - (t/\eta)^2)/(\eta\sqrt{\pi})]\} \end{aligned} \qquad [2]$$

where $t = |\mathbf{r}_{p'} - \mathbf{r}_h - \mathbf{r}_p|$ and

$$G_j(p) = \sum_{i=1}^{3} \{[x^i(p) + h_i - x^i(p')] \cdot \mathbf{a}_i \cdot \mathbf{a}_j/t\},$$

where $\mathbf{a}_j$ is the unit cell vector, $\mathbf{r}_p$ is the position of the p ion, and $x^i(p)|\mathbf{a}_j|$ is the jth contravariant component of $\mathbf{r}_p$, where p is the index of the ions of the unit cell, including lone pairs, and $\mathbf{h}$ is the index of the cells and corresponds in fact to the three indexes h_1, h_2, and h_3, z_p is the p ion relative charge, Δ is the unit cell volume, $k_\mathbf{h} = \sum_{i=1}^{3} h_i a_i^*$ and F is the error function:

$$F(x) = (2/\sqrt{\pi}) \int_0^x \exp(-t^2)\, dt.$$

The prime on the second summation means that $\mathbf{h} \neq 0$ if $p = p'$. Finally, η is the parameter of Ewald's method, homogeneous to a length on the order of the interatomic distances.

The summation convergence speed of Eq. [2] depends on the value of η. Usual values are either half the length of the shorter interatomic distance, or the cubic root of the unit cell volume.

Thus, having calculated the local electric field $E_j(p')$, we obtain the position of the lone pair, defined by the $\boldsymbol{\delta}$ vector, by the relation

$$\delta_j = (\alpha/z|e|)(\mathbf{E}_j(p') + z|e| \cdot \delta_j^{\text{ini}}/|\boldsymbol{\delta}^{\text{ini}}|^3), \qquad [3]$$

where δ_j is the jth covariant coordinate of the $\boldsymbol{\delta}$ vector, α is the electronic polarization coefficient of the ion with the lone pair, z is the relative charge of the lone pair, i.e., -2, and δ_j^{ini} is the arbitrary initial value for δ_j. The second term is introduced here to subtract the contribution of the lone pair associated with the p' ion in the local electric field.

After the calculation of the positions of the lone pairs, we pursued the calculation of the energy of the resulting structure.The total energy is also called the cohesion energy, corresponding to the opposite of the sublimation energy. This energy contains the electrostatic energy of the ionic structure, which can be written as

$$W_{\text{el}} = \frac{1}{2} \sum_{p,p'} \sum_{\mathbf{h}}' z_p z_{p'} |e|^2/t, \qquad [4]$$

where p and p' are the indexes of the unit cell ions, $\mathbf{h}$ is the index of the crystal cells, and $z_p|e|$ and $\mathbf{z}_{p'}|e|$ are the charges of the p and p' ions. The prime on the second summation means that the case $h_1 = h_2 = h_3 = 0$ is excluded when $p = p'$. Using Ewald's method to calculate this energy, we express W_{el} in electron volts as

$$W_{\text{el}} = |e|/(8\pi\varepsilon_0) \sum_{p'} z_{p'} \Phi(\mathbf{r}_{p'}), \qquad [5]$$

where $1/(8\pi\varepsilon_0) = 4.5 \times 10^9$ (USI), and $|e| = 1.602\ 10^{-19}$ C, p' is the index of the ions, including lone pairs, $z_{p'}$ is the p' ion relative charge, and

$$\Phi(\mathbf{r}_{p'}) = \sum_{p} \sum_{\mathbf{h}}' \{[z_p/(\pi\Delta|\mathbf{k}_\mathbf{h}|^2)][\exp(-\pi^2\eta^2|\mathbf{k}_\mathbf{h}|^2)]\cos(2\pi \mathbf{k}_\mathbf{h} \cdot (\mathbf{r}_{p'} - r_p)) + (z_p/t) \cdot [1 - F(t/\eta)]\} - (2z_{p'})/(\sqrt{\pi} \cdot \eta)], \qquad [6]$$

with the same notation as in Eq. [2].

The lone pairs are considered common ions of charge $-2|e|$. However, the interaction between each lone pair and its ion of origin is excluded from the summation because both entities form only one ion.

Furthermore, another part of the cohesion energy is the energy of creation of the lone pairs. It corresponds to the energy needed to divide the ion into two charges, the nucleus-centered charge and the lone pair, i.e., the energy needed for the polarization of the ion. That is why this energy can be approximated by the creation energy of the dipole corresponding to the two charges, i.e.,

$$W_{\text{cre}} = \frac{1}{2} \sum \boldsymbol{\mu}_p \cdot \mathbf{E}_p^{\text{loc}}, \qquad [7]$$

where p is the index of the lone pairs, $\boldsymbol{\mu}_p = \mathbf{z}_p \boldsymbol{\delta}_p$. This is an approximation as the distance $|\boldsymbol{\delta}_p|$ between the nucleus and its lone pair is not negligible.

To those Coulomb-type energies is added a repulsive Pauli-type energy W_{rep}. A usual form of this energy for two ions i and j that are separated by the distance $|\mathbf{r}_{ij}|$ is $A_{ij} \cdot \exp(-B_{ij} \cdot |\mathbf{r}_{ij}|)$, where the empirical constants A_{ij} and B_{ij} depend on the pair of ions (10). Because of its abrupt shape, this repulsive energy at equilibrium, is very small in comparison to the attractive electrostatic energy which then is the main component of the energy of cohesion. In our work, we have calculated the Coulomb-type energy that can be determined exactly but we have determined the repulsive energy only in a purely qualitative way using the approximation

$$W_{\text{rep}} = \frac{1}{2} \sum_{p,p'} \sum_{\mathbf{h}}' K/t^n,$$

with a value of n between 9 and 12.

Finally, we neglect the ionization energies appearing in the transformation of the neutral atoms to ions.

COMPUTERIZATION OF THE LONE PAIRS LOCALIZATION METHOD AND OF THE COHESION ENERGY CALCULATION

We have computerized those calculations of the local electric field and energy on Sun 4-UNIX and PC systems in the standard Pascal language (11). The lattice parameters a, b, c, α, β, γ, the number of atoms in the cell, the relative atomic coordinates, and the charges of the ions are introduced in an input file. The parameters needed for the calculations are also introduced at the same time: the Ewald parameter η (in Å), and the accuracy sought on the position and on the energies. The summations for the calculation of a position or an energy are expanded until the last calculated term is smaller than those precision parameters. Finally, the introduction of the lone pairs is made by defining for each ion possessing a lone pair the electronic polarizability coefficient, the relative charge of the lone pair, which should be -2 but which may be changed if necessary, and the initial position of the lone pair. Let us note here that we introduced the possibility of associating more than one lone pair with an ion, with different charges and a different polarizability coefficient for each lone pair. These charges are named movable charges here, as opposed to the fixed charge on the atomic position. This generalization yields minor modifications in the calculations and may be useful in modeling, for example, multipoles or molecular groups.

All the atoms of a unit cell have to be defined one by one even if they are symmetrically equivalent. Similarly, the calculation of the positions of the lone pairs or of the energetic contributions of the ions are normally made ion by ion even if they possess symmetry relations. So, to reduce the time of calculation, we introduced the possibility of linking charges (lone pairs and ions) that have the same particular Wyckoff's position (and thus the same energetic contribution), so that the calculation of a position or of an energetic contribution need be made only once. We also introduced the possibility of calculating interatomic distances between the ions, including lone pairs.

Ewald's method offers the possibility of easily introducing a Gaussian charge distribution on each ion instead of a punctual charge. Equations [3] and [5] are only slightly modified. It was shown that such distributions have a relevant influence on the electrostatic energy (12). So, we introduced the possibility of associating to each ion a Gaussian charge distribution with a certain full-width half-maximum parameter. This possibility is interesting as it permits the decomposition of ions in a punctual charge composed by the nucleus and the deep electronic layers and a Gaussian charge distribution composed by the external electronic layers, so that the model can better approximate reality.

In addition, in order to study complex structures, we introduced the possibility of defining incommensurate modulations and impurities. A modulation on the atomic positions is introduced by a deviation from the average position of the form

$$u_i = A_i \cos[2\pi\, \mathbf{q}_I \cdot \mathbf{r} + \varphi], \qquad [8]$$

with $i = 1, 2, 3$, $\mathbf{q}_I$ being the incommensurate wave vector and $\mathbf{r}$ determines the average atomic position. But, as Ewald's method is only applicable to crystalline structures, we made it possible to define multiple cells easily from the definition of one cell. Thus, a modulated structure can be approximated by a commensurate structure with a supercell composed of several adjacent unit cells along the modulation direction, while the modulated displacements are applied to the atoms of the supercell (see the application on α-PbO below). In addition, the introduction of impurities can be analyzed by creating a supercell composed of one unit cell containing the impurity and other cells being normal. As the program can support 2000 atoms per unit cell, a sufficiently large supercell can be defined to evaluate the influence of an isolated impurity on its neighborhood.

The program can be applied to other types of structures than those containing lone pairs. A charge distribution containing pure dipoles, for instance, can be processed by this program. The only difference between lone pairs and dipoles is that the latter are composed of two infinitely close charges instead of two charges separated by nonnegligible distances. Thus, the modeling of a dipole introduces two important charges (more than $10|e|$) separated by a very short distance in comparison to other distances of the structure (less than 0.1 Å for instance), so that the total electric dipole moment equal to $z|e|\boldsymbol{\delta}$ gives the desired value. One can either impose fixed values (orientation and intensity) on the electric dipoles, or let them vary according to their electrostatic environments and polarizability coefficients. Regarding the electrostatic energy, the interaction between the two close charges is not taken into account but its dipolar influence is present. As the program permits more than two charges to compose one ion, multipoles can be modeled too. In some complex structures, it may be important to introduce certain delocalized electronic distributions to model the structure (Fig. 1b). With this aim, the program gives the possibility of introducing ions composed of several punctual charges (molecular groups). Interactions between those charges are not taken into account but the electric interactions between all those groups can be estimated. In the same manner iono-covalent bonding can be introduced (Fig. 1c).

The calculation of the electrostatic energy of the charge distribution has been verified for well known values of

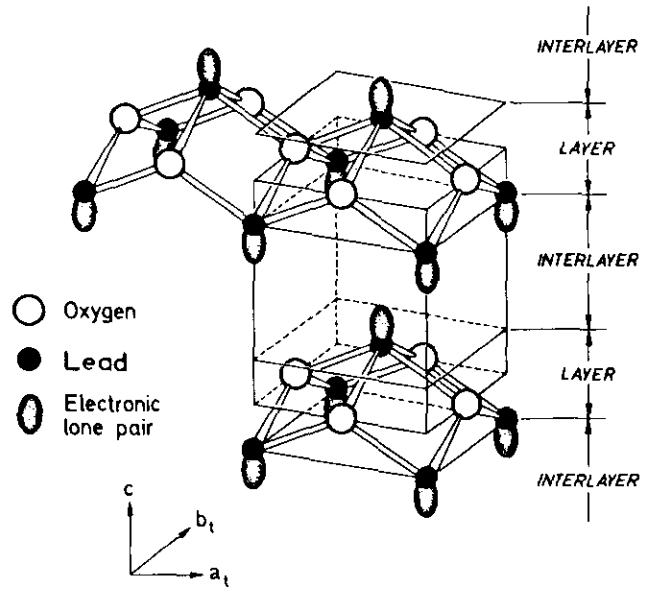

FIG. 2. Room-temperature α-PbO structure. The lone pairs of the Pb^{2+} ions are schematically represented by dashed lobes.

NaCl and CsCl structures. The energies are obtained in a few seconds with a precision of 10^{-5} eV. Other verifications of the energetic calculations have been made with the work of Bertaut (13) on the structure of $RbAlF_4$ in the presence of electric dipoles. We could calculate in a few seconds the different energies in agreement with his results. Regarding the local electric field, we referred to Verbaere *et al.* (1) with calculations on thallium(I) oxygenated compounds and the room temperature structures of α-PbO and β-PbO. Some improvements may be made in the computerization, such as the introduction of polarizability tensors for the polarizable ions. Such improvements should make it possible to investigate more complex structures.

APPLICATION TO THE STUDY OF THE INCOMMENSURATE STRUCTURAL TRANSITION OF α-PbO

We present an application of these calculations in the framework of the study of a structural incommensurate transition that occurs in the tetragonal phase of lead monoxide α-PbO (14–16). Figure 2 shows the very simple layered structure of α-PbO at room temperature. In parallel, we studied the two isostructural compounds, tin monoxide SnO and the solid solution $Pb_{1-x}(TiO)_xO$ with $x \approx 0.06$, where some Pb atoms are substituted by a TiO group. It was shown that α-PbO presents a structural phase transition at 224 K. This transition is characterized by two phenomena: a mono-incommensurate modulation appears along the $[110]^*$- or $[1\bar{1}0]^*$-axis, and a weak ferroelastic distortion distinguishes the directions $\mathbf{a}_0 = \mathbf{a}_t + \mathbf{b}_t$ and $\mathbf{b}_0 = \mathbf{a}_t - \mathbf{b}_t$. This is a displacive-type transition and the low-temperature modulated phase should result from the condensation of a phonon soft mode (16). The modulated structure has been determined from X-ray and neutron powder diffraction results (15, 16). In contrast, SnO and $Pb_{1-x}(TiO)_xO$ do not present any transition and conserve the tetragonal structure until at least 1.5 K. It was shown that lone pairs' interactions are likely to be responsible for the transition in α-PbO. We propose a model showing that the phonon soft-mode condensation in α-PbO can originate from electrostatic interactions between polarized Pb^{2+} ions, leading to structural instability. We show, in agreement with the experimental results, that such interactions are either too weak to induce the transition in SnO or strongly disturbed by the TiO groups in $Pb_{1-x}(TiO)_xO$.

The calculations of the positions of the lone pairs in room- and low-temperature α-PbO structures use structural data obtained by X-ray and neutron powder diffraction (15): that is, the three lattice parameters and the z position of the lead atom in the tetragonal phase. Calculations for the low temperature incommensurate phase require the same parameters in addition to six amplitude and phase modulation coefficients for each two independent atoms, i.e., one lead and one oxygen atom. We introduced the electronic polarizability coefficient for the Pb^{2+} ions: $\alpha = 4.9$ Å^3 (8).

In the tetragonal room-temperature structure, the $\boldsymbol{\delta}$ vectors, defining the positions of the lone pairs in relation to the Pb^{2+} ions site symmetry, are parallel to c_t. The calculation confirms that lone pairs are, in the interlayers, parallel to the c-axis with distance $|\boldsymbol{\delta}| = 0.995$ Å (Table 1). Moreover, a decrease of the a_t-parameter, the c_t-parameter, or the z-parameter induces in the calculation respectively an increase, no variation, or a decrease of $|\boldsymbol{\delta}|$. Experimentally, a decrease of the a_t- and c_t-parameters and an increase of the z-parameter are observed in

TABLE 1
Pb^{II} Lone Pair Localization Calculation Results in the Tetragonal and Incommensurate Phases of α-PbO (Distances in Å)

	Normal phase (300 K)	Incommensurate phase (5 K)			Average structure
		Minimum	Maximum	Average	
$\lvert\boldsymbol{\delta}\rvert$ = Pb–E	0.995	0.952	1.097	1.024	1.008
O–O (along $\mathbf{a}_0$)	2.810	2.803	2.803	2.803	2.803
O–O (along $\mathbf{b}_0$)	2.810	2.728	2.878	2.803	2.803
E–E (along $\mathbf{a}_0$)	2.890	2.815	2.955	2.875	2.870
E–E (along $\mathbf{b}_0$)	2.890	2.782	2.977	2.872	2.870
O–E	2.944	2.873	3.074	2.967	2.951

Note. E represents the lone pair (see also Fig. 2).

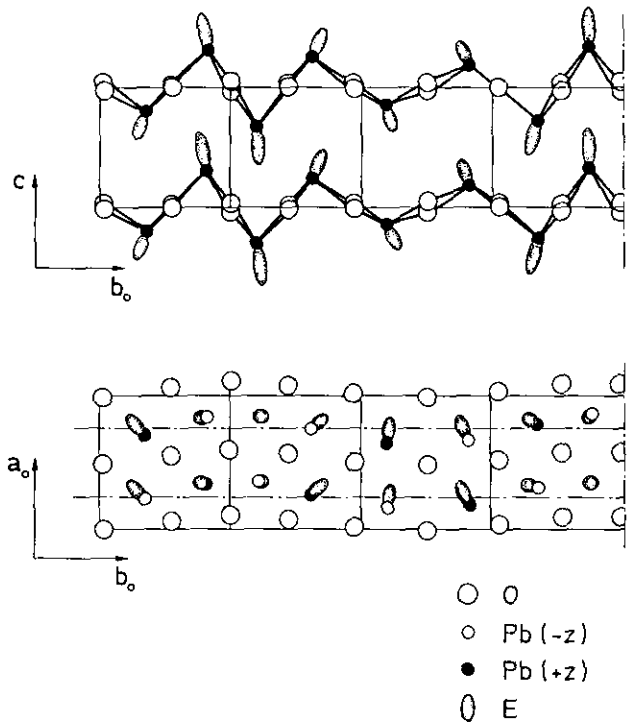

FIG. 3. Schema of the lone pairs' positions in the modulated structure of α-PbO at 5 K. The atomic and lone pair displacement amplitudes are multiplied by a factor of 5.

cooling from room temperature; so the distance $|\delta|$ increases when the temperature decreases. This, in addition to the contraction of the lead–lead distance, induces a diminution of the lone pair–lone pair distance (Table 1). Thus, the electrostatic interactions between lone pairs increase as the temperature decreases.

At lower temperatures, we approximated the incommensurate low-temperature phase by a commensurate structure with modulation parameter $\mathbf{q}_I = \frac{3}{8} = 0.375$ instead of the experimental value $\mathbf{q}_I = 0.370(1)(a_t^* + b_t^*)/2$, using a supercell formed by eight adjacent unit cells (defined by the vectors $\mathbf{a}_0$, $\mathbf{b}_0$, and $\mathbf{c}_0 = \mathbf{c}_t$) along the direction of the modulation. The resulting positions of the lone pairs are presented in Fig. 3. The main result is that the lone pairs are tilted from the c-axis and possess a sort of movement of precession around this axis. In addition, calculations made with the lattice parameters of the incommensurate phase but with no modulation (i.e., the average orthorhombic structure), show that the lone pair–lone pair distances of this structure are practically equal to the average value of that of the incommensurate structure (2.870 Å instead of 2.875 and 2.872 Å, Table 1). But the average distance $|\delta|$ is greater in the modulated structure than in the nonmodulated structure (1.024 instead of 1.008 Å). This shows that the modulation is favorable to the extension of the lone pairs while the lone pair–lone pair distance is kept unchanged, which means that the lone pairs preserve their steric occupation.

We have calculated the energy of the modulated structure taking into account the calculated positions of the lone pairs; a detailed report will be published elsewhere (16). The main result was obtained by varying the modulation parameter $\mathbf{q}_I$ in the electrostatic energy calculation while keeping constant the values for the modulation amplitudes: in that case the energy of the modulated structure is minimized for a value of $\mathbf{q}_I = 0.31$ (Fig. 4), which approximately corresponds to the experimental value $\mathbf{q}_I = 0.370(1)$. This minimum was observed to disappear when the polarizability coefficient α of Pb^{2+} ions diminishes. As the extension of the lone pairs is directly connected to this coefficient, this shows that the instability is created by the presence of the lone pairs in the structure. Moreover, the decomposition of the electrostatic energy into three terms relative to the different interactions, Coulomb-type interactions between punctual charges, interactions between dipoles only, and interactions between punctual charges and dipoles, reveals that it is the interactions between dipoles (i.e., ion–lone pair—ion–lone pair) which are responsible for the minimum in the total curve, and thus for the instability of the structure.

Finally, using our program, we have calculated the electric fields produced by the modulation displacement of a Pb^{2+} ion on its first and second nearest neighbors and show the existence of a frustration which could explain, through the application of an Axial Next Nearest Neighbour Ising model (ANNNI model), the stabilization of the incommensurate phase at temperatures down to 0 K (17).

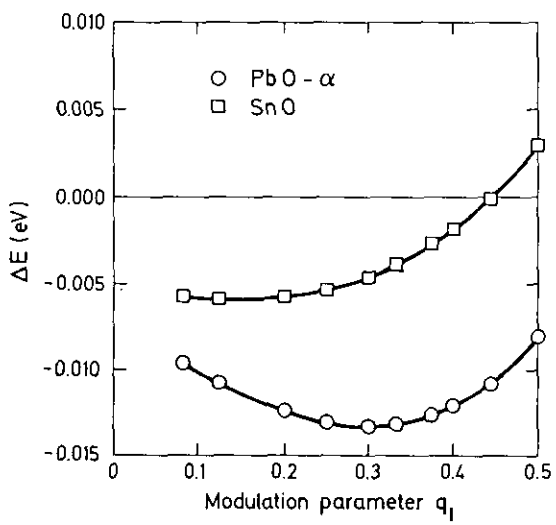

FIG. 4. Electrostatic energy difference per chemical formula between the nonmodulated structure and the modulated structure of α-PbO at low temperatures with a varying modulation parameter $\mathbf{q}_I$. The same curve in the hypothesis of a modulation in SnO.

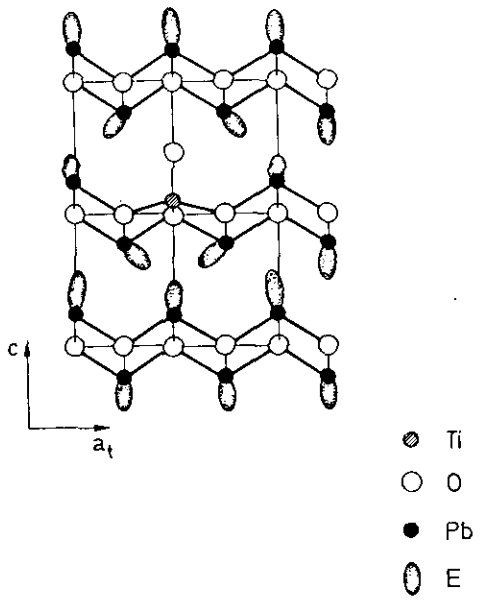

FIG. 5. Schema of the lone pairs' positions perturbed by a TiO group in the structure of α-PbO. The variations of the vectors $|\delta|$ from the average value are multiplied by a factor of 5.

The same calculations have been applied to the SnO and $Pb_{1-x}(TiO)_xO$ structures. In SnO, the lattice and position parameters and the polarizability coefficient of Sn^{2+} ions (α = 4.0 Å^3) are different from those of α-PbO. We find a smaller extension in SnO than in α-PbO, $|\delta|$ = 0.903 Å at room temperature. Moreover, assuming the same type of modulation as in α-PbO, no minimum in the curve of electrostatic energy versus q_l was evidenced contrarily to lead oxide. Figure 5 presents the result of lone pair localization in $Pb_{1-x}(TiO)_xO$ using a supercell of PbO with a substitution of a lead atom with its lone pair by a TiO group. The lone pairs of the lead atoms in the vicinity of the TiO group appear to be greatly displaced: indeed, a tilting of the lone pairs in relation to the c-axis with a maximum amplitude of 13° is observed. These tilts allow a decrease of the interlayer distance as experimentally observed. This local perturbation has as a consequence the diminishing of the interaction which is responsible for the transition in lead oxide, as experimentally shown by the stability of the tetragonal phase down to low temperatures.

APPLICATIONS TO SOME DIFFERENT COMPLEX STRUCTURES

We briefly present three other examples of application of lone pair localization to some compounds its role in whose structural evolutions is qualitatively pointed out. Our results show the applicability of this method to different structures as well as complex structures such as a BiSrCaCuO-type superconductor.

Lead Orthophosphovanadates

The lead orthophosphate $Pb_3P_2O_8$ and the lead orthovanadate $Pb_3V_2O_8$ possess phase transitions from a rhombohedral γ phase at high temperatures to different monoclinic α and β phases (6, 18, 19). The structure of the rhombohedral γ phase is a stacking of PO_4 (or VO_4) tetrahedra layers, orthogonal to the threefold axis (Fig. 6). In a layer, chains of tetrahedra are connected by lead atoms of two types: Pb_1 inside the layers and Pb_2 at the surfaces of the layers. It was shown that the main displacements observed in the phase transitions are movements of lead atoms parallel to the layers of the structure. Those lead atoms possess a lone pair in the interlayer space.

We present a quantitative approach of the determination of the lone pairs' position in the different structures of those compounds. Table 2 shows the different extensions and tilts θ, defined by the angle between the δ vector and the direction of the a^* direction (threefold-axis in the γ phase) perpendicular to the layers. We introduced the ions Pb^{2+}, P^{5+} or V^{5+}, and O^{-2}. It is observed that the

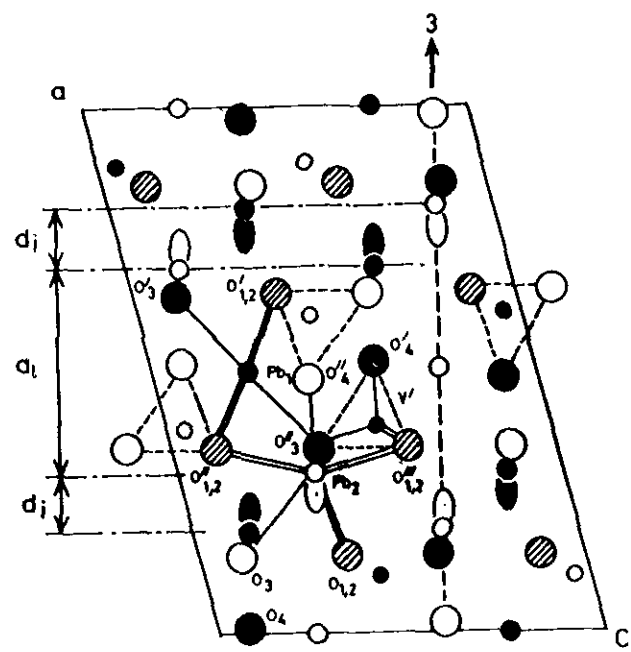

FIG. 6. Projection of the structure of the γ phase of $Pb_3V_2O_8$ in the a, c plane of the monoclinic common cell which can be used to describe the rhombohedral and the low temperature monoclinic phases (the threefold axis is along $\mathbf{a}^*$). The small, medium, and large circles represent respectively the vanadium, lead, and oxygen atoms, and the lobes represent the electron lone pairs. Open circles are located at $y = \frac{1}{4}$, closed circles at $y = \frac{3}{4}$, and hachured circles at $y \approx 0$ and $\approx \frac{1}{2}$. The VO_4 tetrahedra are represented by dashed lines; d_i and d_l are the layer thickness and interlayer distances, respectively (6).

TABLE 2
Pb^{II} Lone Pair Localization Calculation Results in $Pb_3V_2O_8$ and $Pb_3P_2O_8$ Structures (Distances in Å)

	$Pb_3V_2O_8$			$Pb_3P_2O_8$	
	γ-phase (573 K)	β-phase (300 K)	α-phase (85 K)	γ-phase (473 K)	β′-phase (300 K)
Component of δ along **a*** (Å)	0.086	0.049	−0.103	−0.101	−0.065
Component of δ along **b*** (Å)	0	−0.386	−0.248	0	−0.321
Component of δ along **c*** (Å)	0	0.215	0.266	0	0.081
$\|\delta\|$ (Å)	0.086	0.445	0.378	0.101	0.337
Angle θ (**a***, δ)	0°	84°	106°	180°	101°

Note. The angle θ is between the **a*** vector orthogonal to the layer (parallel to the threefold-axis in the γ phase) and δ.

lone pairs occur perpendicular to the layers in the γ phases of both compounds, due to the symmetry of the Pb^{2+} ions' positions. A surprising feature is that the calculated positions of the lone pairs in the γ phase of $Pb_3V_2O_8$ are localized inside the layers instead of occupying the interlayers (tilt $\theta = 0°$); in contrast, the lone pairs occupy the interlayer in $Pb_3P_2O_8$. In the monoclinic phases, the lone pairs are tilted and are nearly parallel to the layers; in the α phase of $Pb_3V_2O_8$ the lone pairs return inside the interlayer. This configuration of strong tilts is obviously favorable to the large shears observed experimentally. Moreover, the different monoclinic phase transitions and the associated shears allows the extension of the lone pairs: $|\delta| = 0.445, 0.378, 0.337$ Å in the β, α, β′, monoclinic phases, instead of 0.086 Å in the γ phase of lead vanadate and 0.101 Å in the γ phase of lead phosphate (Table 2). This shows that the different monoclinic phases that result from the transformation of the common rhombohedral phase differ in the different steric occupation of the lone pairs inside the interlayer.

Minium Pb_3O_4, Comparison with $SnPb_2O_4$

The room temperature structure of the minium Pb_3O_4 is shown in Fig. 7. Two types of polyhedra are present: PbO_6 octahedra (where the lead atoms have a IV valence, thus with no lone pair) and irregular pyramids with a Pb^{II} lead atom at the vertex. In contrast to the other structures described above, the associated lone pairs of the Pb^{II} atoms are expected in this case to occupy the large canal of this structure formed by the Pb^{II} lead ions. At low temperatures Pb_3O_4 presents a sequence of three ferroelastic and ferroelectric transitions from a tetragonal phase at room temperature to orthorhombic phases stable at temperatures below 170 K (20). The structural origin of those transitions was attributed to the steric occupation of the lone pairs of the Pb^{II} ions in the structure. It is

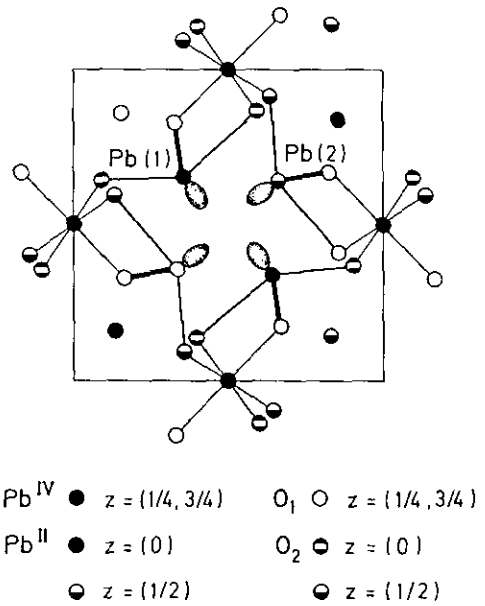

FIG. 7. Projection perpendicular to the *c* tetragonal axis of the Pb_3O_4 structure at room temperature.

interesting to make an analysis of the lone pairs' positions in the different structures using the data from (5). We also determined the lone pairs' positions in the room temperature isostructural $SnPb_2O_4$ compound where no structural transition occurs. The calculations were made with the polarizability coefficients $\alpha(Pb^{2+}) = 4.9$ Å^3 and $\alpha(Sn^{2+}) = 4.0$ Å^3.

The results are presented in Table 3. The lone pairs occupy the canals as expected (Fig. 7). The transition from the room-temperature to the low-temperature structure is characterized by a slight rotation of the lone pairs that reconfigures the occupancy of the canals. In $SnPb_2O_4$ at room temperature and at 5 K, the results show that the lone pairs have an equivalent extension to that in Pb_3O_4 which contradicts the interpretation proposed in (21), that is, a "pumping" process of the lone pairs in those struc-

TABLE 3
Pb^{II} Lone Pair Localization Calculation Results in Pb_3O_4 and $SnPb_2O_4$ (Distances in Å)

		Pb_3O_4		$SnPb_2O_4$	
		300 K	8 K	300 K	8 K
Pb(1)	$\|\delta\|$ (Å)	0.84	0.87	0.91	0.88
	Angle θ (**a**, δ)	28°	25°	21°	24°
Pb(2)	$\|\delta\|$ (Å)	0.84	0.83	0.82	0.85
	Angle θ (**a**, δ)	28°	34°	35°	33°

Note. The angle θ is between the tetragonal **a** vector (see also Fig. 6) and δ.

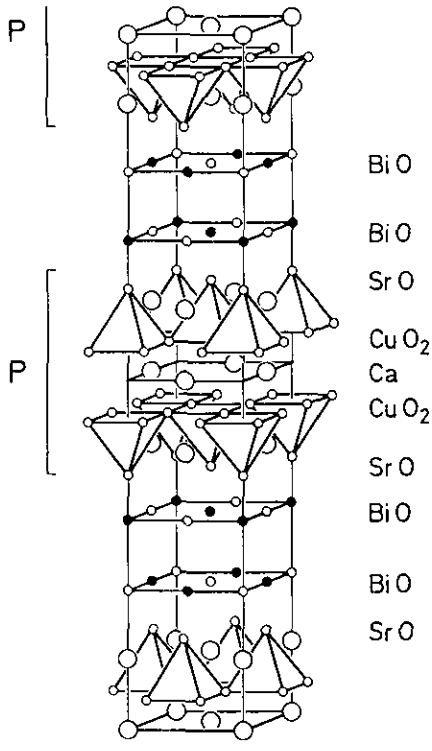

FIG. 8. Structure of the superconductor $Bi_2Sr_2CaCu_2O_8$; P is the perovskite block, connected to the adjacent one by the Bi–O layers.

tures. Nevertheless, one observes that, due to a slight orthorhombic distortion in $SnPb_2O_4$, the lone pairs have the same type of configuration as in Pb_3O_4 at 5 K (compare Pb_3O_4 at 5 K and $SnPb_2O_4$ at 5 K). This seems to show that in $SnPb_2O_4$, with only a slight orthorhombic distortion at room temperature, a stable occupation of the canals by the lone pairs occurs whatever the temperature is (this is due to lower interatomic distances), in contrast to Pb_3O_4, which needs a more significant structural transition to acquire its low temperature stable state.

A BiSrCaCuO-Type Superconductor

The last example we present is the case of a high-critical-temperature superconductor: $Bi_2Sr_2CaCu_2O_8$. Figure 8 shows the well-known structure with the perovskite blocks and the two Bi–O connecting layers. This compound presents an incommensurate modulation with some modulation amplitudes as large as 0.5Å, and there are 60 atoms in the unit cell. Its structure has been determined by several authors. To our knowledge the most complete data are at present those of Kan and Moss (22). The Bi^{3+} ions have electronic lone pairs which should occupy the interlayers between adjacent Bi–O layers; the role of the lone pairs in incommensurate modulation has often been pointed out (7). We have performed the localization of these lone pairs, using the polarizability coefficient $\alpha(Bi^{3+}) = 3.0$ Å^3 obtained from the Clausius–Masotti formula and refraction indexes of several Bi^{3+} ion-containing compounds. In order to introduce the modulation with $\mathbf{q}_I = 0.212$ we used a 14th-multiple cell with three periods of modulation, i.e., $\mathbf{q}_I = 3/14 \approx 0.214$.

The result of the calculation is presented in Fig. 9. The main result is that the lone pairs' positions change drastically along the modulation direction, in contrast to the case of the incommensurate phase of lead oxide. Indeed, the distances $|\delta|$ between Bi^{3+} ions and their lone pairs change from 0.21 to 1.92 Å. Moreover some lone pairs acquire so strong a tilt that they become parallel to the layers. It is interesting to relate this result to some hypotheses made by Tolédano *et al.* (7) regarding lead-substituted (Bi,Pb)SrCaCuO-type compounds. In those compounds, the modulation could be due to the Pb^{2+} lone pairs being parallel to the layers. This shows that this configuration of the lone pairs also exists in non-lead-substituted compounds, perhaps giving some clue to the origin of the incommensurate modulation in this system.

Finally, comparison with the structure of lead oxide and that of the compound $Pb_{1-x}(TiO)_xO$ suggests the examination of the incommensurate and structural characteristics of $Bi_2Sr_2CaCu_2O_8$ compounds doped with titanium: indeed, a recent study (23) has shown that no variation in the superconductor critical temperature is observed when titanium is substituted for bismuth (even for high concentrations up to 50%). The advantage of such a substitution could be that large single crystals could be

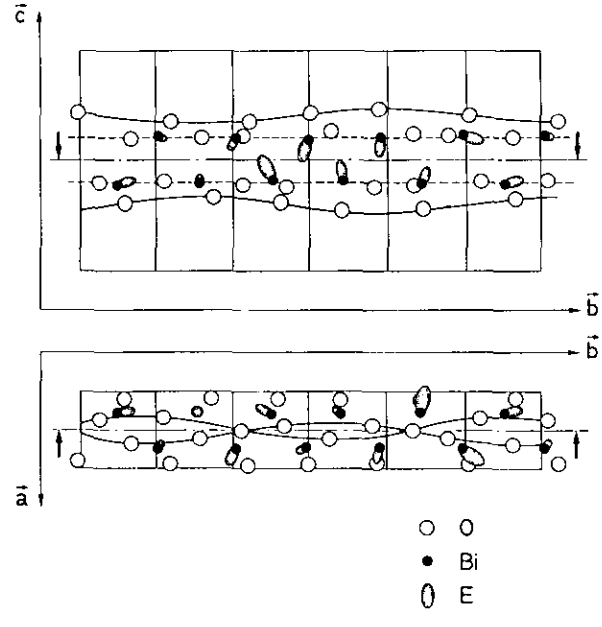

FIG. 9. Lone pair localization in $Bi_2Sr_2CaCu_2O_8$. Dashed lines show the BiO planes.

more easily grown, as observed for $Pb_{1-x}(TiO)_xO$ compared with α-PbO, because in these structures a TiO group replaces a lead (bismuth) atom with its lone pair, which results in an increased coherence between layers.

CONCLUSION

Using a very simple model of punctual charge distribution we have performed lone pair localization and electrostatic energy calculation in various structures. In the case of α-PbO this method allowed the explanation of the origin and stability of the incommensurate phase at low temperature, which is due to dipolar interactions between lead atoms, and the understanding of the absence of transitions in isotypic compounds SnO and $Pb_{1-x}(TiO)_xO$. This method has been applied to some other lead oxides, in particular to minium, Pb_3O_4, for which the lone pairs have been shown to occupy the large canals of the structure. The method has also been shown to be applicable to complex structures such as BiSrCaCuO-type superconductors with 60 atoms per unit cell and elevated amplitude incommensurate modulations.

A general result is that electrostatic interactions between lone pairs have great importance for the occurrence or absence of phase transformation in these types of compounds. In the case of lead oxide and isotypic compounds it is interesting to observe that using a crude ionic model, predictions for the presence or absence of phase transformation in these very simple structures are achieved; therefore we suggest that more sophisticated methods such as ab initio and first principle calculations could easily be applied with profit to such compounds.

REFERENCES

1. A. Verbaere, R. Marchand, and M. Tournoux, *J. Solid State Chem.* **23,** 383 (1978).
2. J. Galy, G. Meunier, S. Andersson, and A. Åström, *J. Solid State Chem.* **13,** 142 (1975).
3. B. Darriet, J. O. Bovin, and J. Galy, *J. Solid State Chem.* **19,** 205 (1976).
4. A. Watanabe, *Mater. Res. Bull.* **19,** 877 (1984).
5. J. R. Gavarri, D. Weigel, and A. W. Hewat, *J. Solid State Chem.* **23,** 327 (1978).
6. J. M. Kiat, P. Garnier, G. Calvarin, and M. Pinot, *J. Solid State Chem.* **103,** 490 (1993).
7. J. C. Tolédano, J. Schneck, and L. Pierre, "Geometry and Thermodynamics" (J. C. Toledano, Ed.), p. 335. Plenum Press, New York, 1990.
8. J. R. Tessman, A. H. Kan, and W. Shockley, *Phys. Rev.* **92**(4), 890 (1953).
9. M. P. Tosi, *Solid State Phys.* **16,** 1 (1974).
10. C. Kittel, "Physique de l'état solide," 5th ed., Dunod, Paris, 1983.
11. This program is available from the authors upon request.
12. J. Birman, *Phys. Rev.* **97**(4), 897 (1955).
13. E. F. Bertaut, *C.R. Seances Acad. Sci. Ser. 2* **302**(6), 285 (1986).
14. J. Moreau, J. M. Kiat, P. Garnier, and G. Calvarin, *Phys. Rev. B* **39**(14), 10296 (1989).
15. A. Hédoux, D. Grebille, and P. Garnier, *Phys. Rev. B Condens. Matter* 40(15), 10653 (1989).
16. D. LeBellac, J. M. Kiat, P. Garnier, A. Moudden, M. Pinot, G. André, M. P. Buffat, and Ph. Sciau, to be published.; D. LeBellac, Thesis, Université d'Orsay, unpublished, 1993.
17. C. Benkert,V. Heine, and E. H. Simmons, *Europhys. Lett.* **3**(7), 833 (1987).
18. J. M. Kiat, Y. Yamada, G. Chevrier, Y. Uesu, P. Boutrouille, and G. Calvarin, *J. Phys. C* **4,** 4915 (1992).
19. J. M. Kiat, G. Calvarin, and Y. Yamada, *Phys. Rev. B Condens. Matter* 48, **1,** 34 (1993).
20. P. Garnier, G. Calvarin, and D. Weigel, *J. Solid State Chem.* **16,** 55 (1976).
21. J. R. Gavarri, J. P. Vigouroux, G. Calvarin, and A. W. Hewat, *J. Solid State Chem.* **36,** 81 (1981).
22. X. B. Kan and S. C. Moss, *Acta Crystallogr. Sect. B* **48,** 122 (1992).
23. N. Yoshitake, N. Kazuoo, K. Takuya, K. Yuichiro, and O. Kazuya, *Phys. Lett. A* **163,** 465 (1992).